JOURNAL OF THE ROYAL SOCIETY Interface

J. R. Soc. Interface (2009) **6**, 271–277
doi:10.1098/rsif.2008.0225
Published online 22 July 2008

Preparation of suspensions of phospholipid-coated microbubbles by coaxial electrohydrodynamic atomization

U. Farook, E. Stride and M. J. Edirisinghe*

Department of Mechanical Engineering, University College London, Torrington Place, London WC1E 7JE, UK

The use of phospholipid-coated microbubbles for medical applications is gaining considerable attention. However, the preparation of lipid-coated microbubble suspensions containing the ideal size and size distribution of bubbles still represents a considerable challenge. The most commonly used preparation methods of sonication and mechanical agitation result in the generation of polydisperse microbubbles with diameters ranging from less than 1 μm to greater than 50 μm. Efforts have been made via distinctly different techniques such as microfluidic and electrohydrodynamic bubbling to prepare lipid-coated microbubbles with diameters less than 10 μm and with a narrow size distribution, and recent results have been highly promising. In this paper, we describe a detailed investigation of the latter method that essentially combines liquid and air flow, and an applied electric field to generate microbubbles. A parametric plot was constructed between the air flow rate (Q_g) and the lipid suspension flow rate (Q_l) to identify suitable flow rate regimes for the preparation of phospholipid-coated microbubbles with a mean diameter of 6.6 μm and a standard deviation of 2.5 μm. The parametric plot has also helped in developing a scaling equation between the bubble diameter and the ratio Q_g/Q_l. At ambient temperature (22°C), these bubbles were very stable with their size remaining almost unchanged for 160 min. The influence of higher temperatures such as the human body temperature (37°C) on the size and stability of the microbubbles was also explored. It was found that the mean bubble diameter fell rapidly to begin with but then stabilized at 1–2 μm after 20 min.

Keywords: phospholipid; coaxial electrohydrodynamic atomization; microbubbles

1. INTRODUCTION

Suspensions of surfactant and polymer-coated microbubbles have gained considerable attention in a range of medical applications, e.g. as ultrasound (US) contrast agents, drug and gene delivery vehicles and blood substitutes (Stride *et al.* 2008). The use of amphiphilic molecules, particularly phospholipids, as coating materials has the particular advantage of being self-assembled around the gas core, providing a strong shell surface architecture suitable for the addition of functional molecules (Borden & Longo 2002; Raisinghani & DeMaria 2002; Stride & Saffari 2003). In this study, we have used a combination of a phospholipid (L-α-phosphatidylcholine) and an emulsifier to aid lipid dispersion and prevent microbubble coalescence (Borden & Longo 2002; Borden *et al.* 2004*a*,*b*).

The most common method for the preparation of lipid-coated microbubble suspensions is agitation and/or sonication. Although sonication enhances the structure of the surfactant monolayer and makes the microbubbles extremely stable, a high level of control over the microbubble size distribution cannot be achieved in this way (Wang *et al.* 1996; Borden *et al.* 2004*b*; Unger *et al.* 2004). Efforts have been made to prepare microbubbles suitable for medical applications using microfluidic devices (Talu *et al.* 2006; Pancholi *et al.* 2008), and it has recently been reported that phospholipid-coated microbubbles suitable for US imaging can be successfully produced via this technique (Hettiarachchi *et al.* 2007). The essential requirement is the control of size and size distribution of the stable microbubbles in order to prepare near-monodisperse microbubbles in the size range of 2–10 μm. However, the simplicity of the design and construction of equipment and the ease of operation and flexibility have motivated us to develop an electrohydrodynamic method of microbubbling as a viable alternative to microfluidic procedures for the preparation of phospholipid-coated microbubbles for US imaging and drug delivery. Conventionally, electrohydrodynamic atomization is used to generate droplets of liquids, a few micrometres in diameter. Recently, using a model glycerol–air system, we reported a new technique, coaxial electrohydrodynamic atomization (CEHDA) microbubbling, which can be successfully used to

*Author for correspondence (m.edirisinghe@ucl.ac.uk).

Received 27 May 2008
Accepted 23 June 2008

prepare suspensions containing microbubbles of less than 10 μm in diameter with a narrow size distribution (Farook *et al.* 2007*a*,*b*). Subsequently, we extended this capability of CEHDA microbubbling for the preparation of polymeric microcapsules with a mean diameter of 6 ± 2 μm using a solution of water-insoluble polymethylsilsesquioxane (Farook *et al.* 2008).

The aim of this paper is to describe a detailed investigation of a lipid–air system for the preparation of near-monodisperse microbubbles of less than 10 μm in diameter, in particular the relationship between microbubble characteristics and the air and lipid suspension flow rates for a fixed applied voltage.

2. MATERIALS AND METHODS

The lipid suspension was prepared by mixing 0.25 g of hydrogenated L-α-phosphatidylcholine, $C_{40}H_{80}NO_8P$ (relative molecular mass 734, purity > 99%; Avanti Polar Lipids, USA), 0.071 g of polyethylene glycol 40 stearate-40 (density 1300 kg m^{-3}; Sigma-Aldrich Co. Ltd, UK), 5 ml of glycerol (density 1260 kg m^{-3}; Sigma-Aldrich Co. Ltd) and 25 ml of propane-1,3-diol (density 1000 kg m^{-3}; Sigma-Aldrich Co. Ltd) in a conical flask containing 50 ml of distilled water with slow magnetic stirring. The flask was then topped up with distilled water up to the 250 ml mark and the mixture was stirred for a further 300 s. The dispersion of the phospholipids was achieved by sonicating the suspension using a Misonix ultrasonic cell disruptor XL200 (Labcaire Systems Ltd, Somerset, UK) operating at 12 W for 60 s. The sonicator probe was placed deep in the suspension to avoid the generation of gas bubbles. To ensure the homogeneous dispersion of the lipid in the suspension, a smaller volume of the suspension was transferred to a test tube and was sonicated in the same manner for 120 s before removing 6 ml of the samples for the preparation of CEHDA microbubbles.

The lipid suspension was characterized at atmospheric pressure and ambient temperature to determine its density, viscosity, surface tension and electrical conductivity. The density was measured using a standard 25 ml specific gravity bottle. The viscosity was estimated by using a VISCOEASY rotational viscometer and the electrical conductivity was measured using a standard conductivity probe. The surface tension was measured using a Kruss tensiometer (plate method). The viscosity and the density of the air were taken as 1.8×10^{-2} mPa s and 1.2 kg m^{-3}, respectively, as reported in standard data books.

The experimental set-up used for CEHDA is shown in figure 1; it is easy to assemble and simple to operate. The coaxial nozzle is made up of an inner stainless steel capillary needle (inner diameter 150 μm and outer diameter 300 μm) carrying the air flow surrounded by an outer stainless steel needle (inner diameter 685 μm and outer diameter 1100 μm) carrying the lipid suspension. The tip of the inner needle was positioned approximately 2 mm inside the outer needle to facilitate air encapsulation by the lipid suspension. Both the needles were connected to the same power supply (Glassman Europe Limited, Bramley, UK).

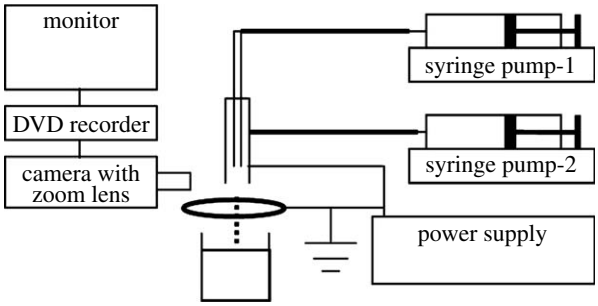

Figure 1. Schematic of the experimental set-up used for coaxial electrohydrodynamic microbubbling.

A ring (inner diameter 15 mm and outer diameter 20 mm) placed approximately 12 mm below the tip of the outer needle acts as the supporting electrode and is also earthed (kept at zero potential). The flow rates of the air and the lipid suspension through the needles were controlled by high-precision Harvard syringe pumps (Harvard Apparatus Ltd, Edenbridge, UK). The capacity of the syringes used for the air and lipid suspensions was 10 and 5 ml, respectively. The flow of the material exiting the needles was observed/recorded using a LEICA S6D JVC-colour video camera attached to a zoom lens and a data DVD video recorder MP-600 using CDV Recorder/Editor DN-100 with a video screen for real-time monitoring. For microscopic examinations, microbubbles were collected 12 mm below the ring electrode in a glass vial containing distilled water.

The air flow rates considered for this study ranged from 8.0 to 0.8 μl s^{-1}. For each value of the air flow rate, the threshold values of intermittent microbubbling (Farook *et al.* 2007*b*) and continuous microbubbling (Farook *et al.* 2007*b*) were noted by gradually increasing the suspension flow rate, observing the transition through the modes of microbubbling (Farook *et al.* 2007*b*) on the video screen. The applied voltage was maintained at 6.1 kV throughout this study. In this way, a parametric map between the air and suspension flow rates was constructed.

Lipid-coated microbubbles were studied by optical microscopy at ambient temperature (22°C), as well as at the human body temperature (37°C). At ambient temperature, 6 ml of the lipid suspension was microbubbled while collecting the microbubble suspension in a glass vial containing 2 ml of distilled water. A sample of 0.05 ml of the microbubble suspension was immediately transferred using a 1 ml syringe from the glass vial to a glass slide and optical microscopic examinations were conducted. The experiments on the behaviour of microbubbles prepared by CEHDA at 37°C were conducted in two stages. First, a glass vial containing 1 ml of distilled water was placed on a hot plate below the ring electrode and the temperature of the distilled water was maintained at 37°C while microbubbling only 3 ml of the lipid suspension into the glass vial. The amounts of distilled water and the lipid suspension were halved to minimize errors during these experiments. However, the bubble concentration was kept constant in all experiments by standardizing the lipid suspension, water volumes and the injection time. After

microbubbling, the vial was removed to ambient conditions and then samples of 0.05 ml were taken at 10, 20, 30, 40, 50 min and after 40 hours for the microscopic examination. Second, 3 ml of the lipid suspension was microbubbled into a glass vial containing 1 ml of distilled water at ambient temperature and then the glass vial was transferred onto a hot plate and the temperature of the microbubble suspension was maintained at 37°C for an hour while samples of 0.05 ml were taken at a duration of 10, 20, 40 and 50 min for optical microscopy. All the micrographs were prepared using the standard Image-ProPlus software (Media Cybernetics, L.P. Del Mar, CA, USA).

In addition to optical microscopy, the microbubble suspensions collected at ambient temperature were also characterized ultrasonically in order to confirm that gas-filled bubbles had been successfully prepared. One millilitre of the microbubble suspension was added to a specially designed chamber filled with distilled water. The chamber was constructed using polymethylmethacrylate tubing (inner diameter 60 mm, wall thickness 5 mm and length 30 mm) with acoustic 'windows' made from a polyethylene film (thickness 50 μm) at either end. The tubing was held between two square aluminium plates into which recessed circular holes had been cut to hold the tubing in place. The chamber was suspended in a water bath, also filled with distilled water, to enable the transmission of the US through the chamber and to minimize temperature fluctuations.

The measurement of US attenuation through the microbubble suspension in the chamber was made using a custom-made broadband transducer having a nominal centre frequency of 1 MHz, a diameter of 20 mm and a 3 dB bandwidth of 60%. This was aligned coaxially with the chamber 20 mm from one of the windows of the chamber so that the US beam passed through the chamber onto a stainless steel reflector and back to the transducer. The distance between the transducer face and the steel plate was 60 mm. The transducer was activated using a pulser/receiver unit (Panametrics model 5055 PR), which was set to give an output peak-negative pressure in water of approximately 50 kPa. The signal capture was performed using a digital oscilloscope (LeCroy 9310M Dual 300 MHz), which was connected via a general-purpose interface bus to a computer. Subsequent data analysis was performed using Matlab (v. 7 of 2006, The Mathsworks, Natick, MA, USA).

3. RESULTS AND DISCUSSION

The measured properties of the phospholipid suspension are given in table 1. These are important since the suspension acts as the driving liquid during the CEHDA process. Viscosity and electrical conductivity play a major role, as these properties are responsible for the electrical charge transport through the liquid mass and for the formation of the cone jet, which determines the final size distribution of the sprayed product (Jayasinghe & Edirisinghe 2002; Ku & Kim 2002; Loscertales *et al.* 2002; Lopez-Herrera *et al.* 2003).

Table 1. Properties of the lipid suspension prepared for the microbubbling experiments.

density	1030 kg m^{-3}
viscosity	2.6 mPa s $\pm$ 1.90%
surface tension	43 mN m^{-1} $\pm$ 0.46%
electrical conductivity	8.8 μS m^{-1} $\pm$ 11.40%

In this process, microbubbling succeeds the dripping of larger bubbles and subsequent narrowing or coning of the liquid stream. The bubble dripping, coning and microbubbling modes observed during CEHDA of the air–lipid system are shown in figure 2*a–c*, respectively. The evolution of these modes is discussed in detail in Farook *et al.* (2007*b*). With the increase in the applied voltage and hence the increase in the magnitude of the electric field, the bubble dripping mode transforms to the microbubbling mode via the coning mode. For the lipid–air system used in this study, the bubble dripping mode was observed between 0 and 2.5 kV. The coning mode exists between 2.5 and 5.7 kV and the microbubbling mode was observed between 5.7 and 6.1 kV. However, in these experiments, microbubbling and sample collection were conducted at 6.1 kV, as this was found to produce the thinnest jet and hence the smallest bubbles.

The aim in measuring the attenuation of US through the prepared suspensions was to determine whether the gas-filled microbubbles were present or not. The attenuation coefficient in a bubbly liquid is significantly higher than in a suspension of solid or liquid particles due to the large acoustic impedance contrast between liquid and gas and the high compressibility of gas bubbles (Stride & Saffari 2005). Hence, this proves a way of confirming the presence of microbubbles independent of using microscopical techniques. Figure 3 shows the frequency spectra for US pulses transmitted through water and the suspension prepared by CEHDA. The large reduction in the signal amplitude for the latter confirms the presence of air-filled microbubbles in the suspension.

The parametric plot constructed between the air flow rate and the flow rate of the lipid suspension is shown in figure 4*a*. A horizontal straight line in the plot shows the level of the critical minimum air flow rate, $(Q_a)_{min}$. There is no microbubbling in zone 1 below the critical minimum air flow rate due to the dominance of the suspension flow. Similarly, zone 2 shows no microbubbling due to the dominance of the air flow. Zones 3 and 4 show intermittent and continuous microbubbling, respectively. Table 2 shows the bubble size distribution obtained for five different combinations of flow rates selected from the parametric plot on a downward vertical line AB (figure 4*a*), corresponding to a suspension flow rate of 5 μl s^{-1}. With the decrease in the air flow rate, a significant decrease in the bubble diameter is achieved. The smallest bubble diameter was obtained only at a flow rate combination, 5 μl s^{-1} : 5 μl s^{-1}, within the intermittent microbubbling zone just below the threshold of continuous microbubbling. Figure 4*b* shows the optical

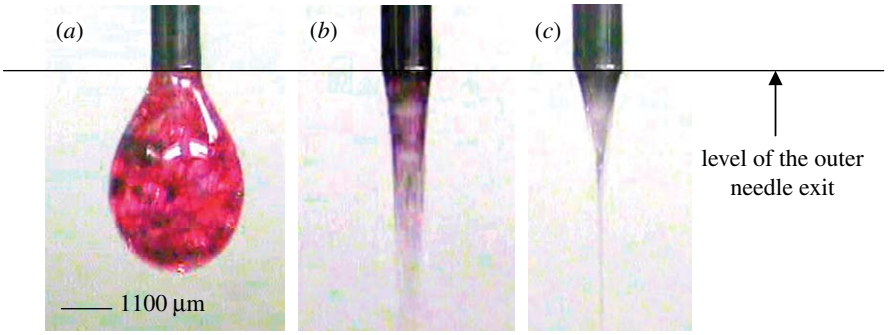

Figure 2. Modes of microbubbling, (*a*) bubble dripping mode, (*b*) coning mode and (*c*) microbubbling mode, observed for the phospholipid suspension.

micrograph of the microbubbles prepared at this flow rate combination. However, it is noteworthy that the smallest size achieved within the continuous microbubbling zone, i.e. zone 4, at a flow rate combination of 10 µl s^{-1} (air) : 5 µl s^{-1} (lipid suspension) also satisfies the requirements in terms of the bubble size for intravenous use (less than 8 µm in diameter). Figure 4*c* shows an optical micrograph of the microbubbles prepared at the flow rate combination of 10 µl s^{-1} : 5 µl s^{-1} (air : lipid).

In figure 5, the continuous microbubbling zone of the air–lipid system has been compared with that of the model air–glycerol system (Farook *et al.* 2007*b*). Curve L represents the onset of continuous microbubbling of the air–lipid system. Similarly, curve G represents results of the air–glycerol system. In the case of the latter, continuous microbubbling begins at lower values of the air flow rate, whereas for the lipid suspension, continuous microbubbling begins at higher air flow rates. The reason for this shift is the difference in physical properties, such as viscosity, surface tension and dielectric behaviour between glycerol and the lipid suspension, and as such this plot is material specific. The applied voltage necessary for the microbubbling mode also therefore varies from system to system.

The microbubbling time for a 6 ml lipid suspension was 20 min and the microbubbles were collected in a glass vial containing 2 ml of distilled water to make the total volume to 8 ml. The reduction in bubble size with the reduction in the gas flow rate at a constant lipid suspension flow rate indicated in table 2 agrees with the previous observations in microbubbling by both microfluidic techniques and CEHDA for other liquids (Ganan-Calvo 2004; Garstecki *et al.* 2005; Farook *et al.* 2007*b*).

For microbubbling in microfluidic flow-focusing systems, Ganan-Calvo (2004) put forward equation (3.1) for liquids with the Reynolds number in the range of 40–1000,

$$d_b = 1.1 D \lambda^{0.4}, \tag{3.1}$$

where d_b is the microbubble diameter (in µm) and the gas ratio $\lambda = Q_g/Q_l$; Q_g and Q_l are the air and liquid flow rates, respectively. D is the orifice diameter.

Interestingly, within the continuous microbubbling zone (zone 4), the mean microbubble diameter d_b, for the air–lipid suspension system, scales with the gas

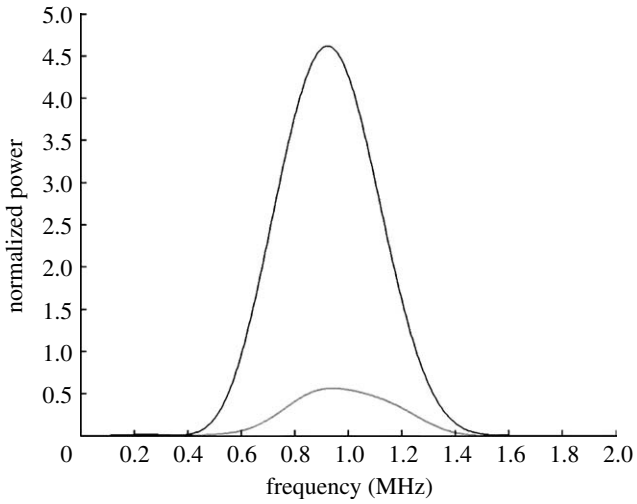

Figure 3. Frequency spectra for a 1 MHz US pulse transmitted through water (black curve) and the CEHDA microbubble suspension (grey curve).

constant λ according to the equation (figure 6)

$$d_b = 5.95 \lambda^{0.14}. \tag{3.2}$$

There are a number of similar features between microbubbling in microfluidic flow-focusing systems and CEHDA microbubbling. For example, d_b decreases with the decrease in λ and with the decrease of D in microfluidic systems or jet diameter (D_j) in CEHDA. However, in CEHDA microbubbling, the change in d_b due to the variation in λ is small (table 2), and this helps to increase the bubble generation frequency. The essential feature in CEHDA is the importance of the parametric plot between the gas flow rate and the liquid (or suspension) flow rate as suitable combinations of these two parameters should be chosen in order to achieve continuous microbubbling. In addition to this, a thin jet at a higher applied voltage helps to decrease D_j and d_b.

The microbubble production rate of this device is approximately 10^9 bubbles min^{-1} for the mean bubble diameter of 6.6 µm. This is more than an order of magnitude higher than that of lithographically prepared flow-focusing microfluidic devices (Hettiarachchi *et al.* 2007). However, the polydispersivity index (s.d./mean expressed as a percentage) of the bubbles prepared is in the range of 30–40 (table 2), whereas in the case of flow-focusing microfluidic devices, this index can be

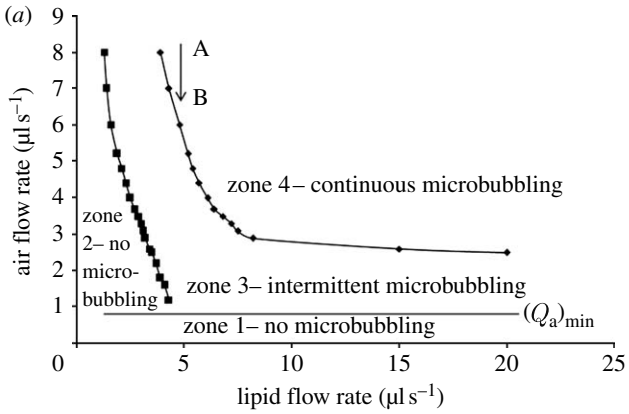

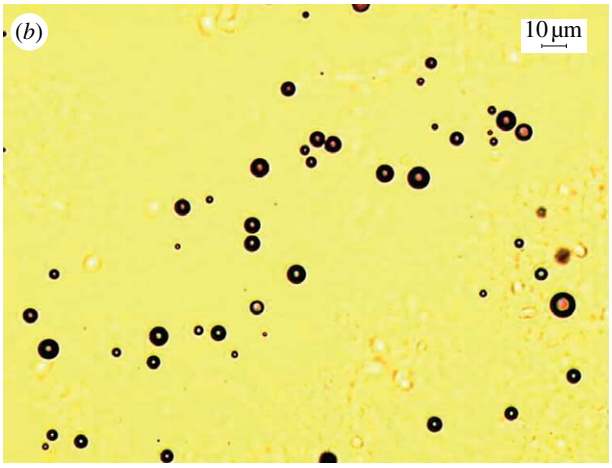

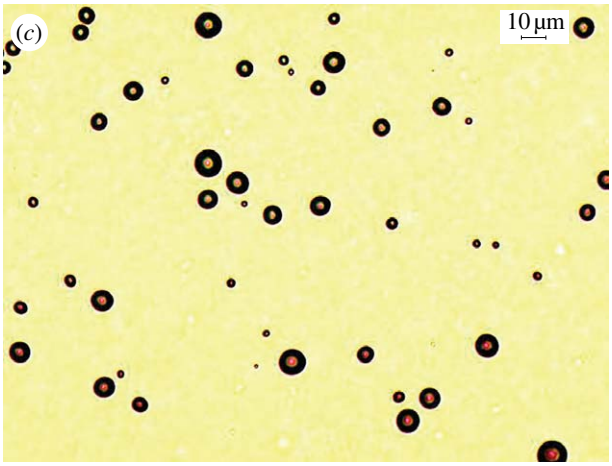

Figure 4. (*a*) A parametric plot between the air flow rate and the flow rate of the lipid suspension to show the onset of microbubbling. Zones 1 and 2, no microbubbling; zone 3, intermittent microbubbling; zone 4, continuous microbubbling. AB is a downward straight line corresponding to a lipid suspension flow rate of 5 µl s^{-1}. (*b*,*c*) Optical micrographs of lipid-coated microbubbles collected at ambient temperature at a flow rate combination of (*b*) 5 µl s^{-1} : 5 µl s^{-1} and (*c*) 10 µl s^{-1} : 5 µl s^{-1}.

less than 2 per cent. Nevertheless, as explained by Hettiarachchi *et al.* (2007), these microfluidic devices suffer from the scenario that high gas pressures and liquid flow rates needed to speed up the bubble production rates result in a significant increase in the polydispersivity index (more than 50%), whereas, in the electrohydrodynamic device used in the present study, the variation in the air and liquid flow rates (figure 4; table 2) does not result in a dramatic change in the polydispersivity index during continuous microbubbling. The polydispersivity index of the microbubbles generated by the electrohydrodynamic device can be further improved by optimizing the geometry of the needles to control the electric field more suitably and we are currently exploring this.

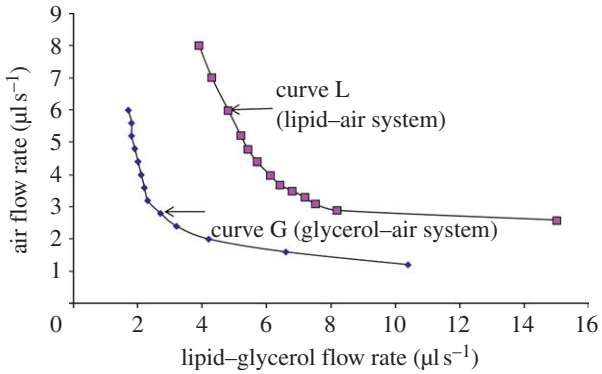

Figure 5. A comparison of the onset of continuous microbubbling in the air–lipid system and the model air–glycerol system.

Table 2. Microbubble sizes obtained by coaxial electrohydrodynamic flow at 22°C. (For the calculation of mean diameters and standard deviations, 100 bubbles were taken from the respective micrographs.)

	flow rates (µl s^{-1})			bubble diameter (µm)	
zones from figure 4*a*	air	lipid	gas ratio (λ)	mean	s.d.
zone 4	25	5	5	7.5	2.4
	20	5	4	7.1	2.7
	15	5	3	6.8	2.1
	10	5	2	6.6	2.5
zone 3	5	5	1	5.5	1.8

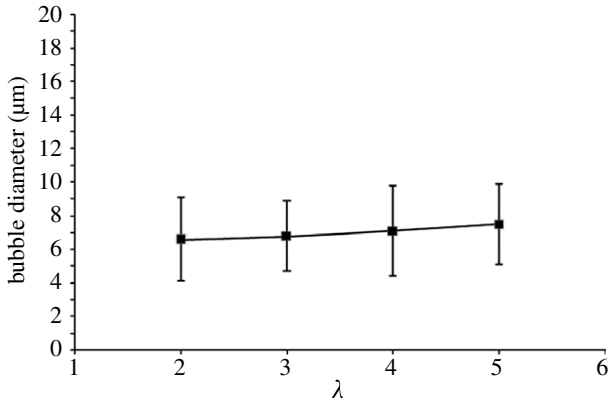

Figure 6. A graph of the microbubble diameter versus the gas ratio (λ) for the air–lipid system within the continuous microbubbling zone.

The stability of the microbubbles prepared at 10 µl s^{-1} : 5 µl s^{-1} (air : lipid suspension) flow rates was evaluated by taking samples for optical microscopy examination at time intervals of 10, 40, 70, 100 and 160 min following collection. The mean bubble

Table 3. Microbubble sizes obtained from the samples collected at 37°C at a flow rate combination of 10 µl s^{-1} (air) : 5 µl s^{-1} (lipid suspension). (For the calculation of mean diameters and standard deviations, 100 bubbles were taken from the respective micrographs.)

	bubble diameter (µm)	
time interval	mean	s.d.
10 min	4.7	1.6
20 min	4.1	1.4
30 min	3.3	1.3
40 min	2.8	1.0
50 min	2.0	1.0
40 hours	1.9	1.0

Table 4. Microbubble sizes obtained from the samples collected and maintained at 37°C at a flow rate combination of 10 µl s^{-1} (air) : 5 µl s^{-1} (lipid suspension). (For the calculation of mean diameters and standard deviations, 100 bubbles were taken from the respective micrographs.)

	bubble diameter (µm)	
time interval (min)	mean	s.d.
10	2.1	0.7
20	1.7	0.6
40	1.3	0.5
50	1.3	0.4

diameter 10 min after preparation was 6.6 µm with a standard deviation of 2.5 µm. After 160 min, the bubble diameter was 6 µm with a standard deviation of 1.8 µm. The effect of different shell materials and gases in the bubble core upon stability has been investigated previously (Soetanto & Chan 2000; Klibanov *et al.* 2002; Krasovitski & Kimmel 2006). However, there have been relatively few *in vitro* investigations of the stability of microbubbles at the human body temperature (37°C). Table 3 shows the size variations of microbubbles prepared at 37°C of the samples taken up to 40 hours after preparation. The relevant micrographs of these samples were taken after allowing the microbubble suspension to cool to ambient temperature. The results show that, within 50 min, the mean microbubble size drops rapidly to 2 µm but then this size is retained for a very long period of time.

Table 4 shows the size variations of microbubbles maintained at 37°C up to 50 min after preparation. The relevant micrographs of these samples were taken while maintaining the microbubble suspension at 37°C. These results indicate that at 37°C, the microbubble size rapidly decreases to a mean diameter of approximately 2 µm and, subsequently, the reduction in size is much slower. Thus, a stable microbubble diameter of 1–2 µm has been achieved and this compares well with the stable microbubble sizes prepared using other techniques such as flow-focusing microfluidics (Talu *et al.* 2006), agitation/sonication (Borden *et al.* 2007) and selective acoustic pulsing (Borden *et al.* 2005).

The size reduction of the lipid-coated microbubbles at 37°C is potentially significant because the bubbles' resonance frequency is directly related to their size and it is desirable that this should fall in the range of US frequencies used for medical imaging (1–10 MHz). It is likely that this would be less significant if a higher molecular weight gas such as perfluorocarbon was used instead of air (Krasovitski & Kimmel 2006).

4. CONCLUSIONS

In this paper, we have provided a systematic analysis of the coaxial electrohydrodynamic microbubbling process for the preparation of coated microbubbles for diagnostic and therapeutic applications. The process uses a simultaneous, coaxial flow of a liquid medium, lipid suspension and a gas, in this case air, under the influence of an electric field allowing the lipid to encapsulate air, thus forming bubbles. The parametric plot of the air flow rate and the lipid suspension flow rate is an important tool in selecting the right process control parameters (e.g. flow rate, applied voltage) to prepare microbubble suspensions with the desired size distributions for a particular application. The parametric plot has also helped in developing a scaling equation between the bubble diameter and the gas ratio. We have successfully prepared microbubbles with a mean diameter below the limit of 10 µm for intravenous use and with a narrow size distribution (6.6 ± 2.5 µm). These microbubbles are also stable for over 2.5 hours. At the human body temperature of 37°C, the microbubbles rapidly decrease in size to 1.3 ± 0.4 µm within 50 min.

EPSRC (UK) is gratefully acknowledged for funding this project under platform grant EP/E045839. The Royal Academy of Engineering (UK) is also thanked for supporting the work of E.S.

REFERENCES

Borden, M. A. & Longo, M. L. 2002 Dissolution behaviour of lipid monolayer-coated, air-filled microbubbles: effect of lipid hydrophobic chain length. *Langmuir* **18**, 9225–9233. (doi:10.1021/la026082h)

Borden, M. A., Dayton, P., Zhao, S. & Ferrara, K. W. 2004*a* Physico-chemical properties of the microbubble lipid shell. In *2004 IEEE Int. Ultrasonics, Ferroelectrics, and Frequency Control Joint 50th Anniversary Conference*, pp. 20–23.

Borden, M. A., Pu, G., Runner, G. J. & Longo, M. L. 2004*b* Surface phase behaviour and microstructure of lipid/PEG-emulsifier monolayer-coated microbubbles. *Colloids Surf. B: Biointerfaces* **35**, 209–223. (doi:10.1016/j.colsurfb.2004.03.007)

Borden, M. A., Kruse, D. E., Caskey, C. F., Zhao, S. K., Dayton, P. & Ferrara, K. W. 2005 Influence of lipid shell physiochemical properties on ultrasound-induced microbubble destruction. *IEEE Trans. Ultrason. Ferroelectr. Freq. Control* **52**, 1992–2002. (doi:10.1109/TUFFC.2005.1561668)

Borden, M. A., Caskey, C. F., Little, E., Gillies, R. J. & Ferrara, K. W. 2007 DNA and polylysine adsorption and multilayer construction onto cationic lipid-coated microbubbles. *Langmuir* **23**, 9401–9408. (doi:10.1021/la7009034)

Farook, U., Zhang, H. B., Edirisinghe, M. J., Stride, E. & Saffari, N. 2007*a* Preparation of microbubble suspensions by co-axial electrohydrodynamic atomization. *Med. Eng. Phys.* **29**, 749–754. (doi:10.1016/j.medengphy.2006.08.009)

Farook, U., Stride, E., Edirisinghe, M. J. & Moaleji, R. 2007*b* Microbubbling by co-axial electrohydrodynamic atomization. *Med. Biol. Eng. Comput.* **45**, 781–789. (doi:10.1007/s11517-007-0210-1)

Farook, U., Edirisinghe, M. J., Stride, E. & Colombo, P. 2008 Novel co-axial electrohydrodynamic *in-situ* preparation of liquid-filled polymer-shelled microspheres for biomedical applications. *J. Microencapsul.* **25**, 241–247 (doi:10.1080/02652040801896666)

Ganan-Calvo, A. M. 2004 Perfectly monodisperse microbubbling by capillary flow focusing: an alternate physical description and universal scaling. *Phys. Rev. E* **69**, 027 301–027 303. (doi:10.1103/PhysRevE.69.027301)

Garstecki, P., Ganan-Cavo, A. M. & Whitesides, G. M. 2005 Formation of bubbles and droplets in microfluidic systems. *Bull. Pol. Acad. Tech.* **53**, 361–372.

Hettiarachchi, K., Talu, E., Longo, M. L., Dayton, P. A. & Lee, A. P. 2007 On-chip generation of microbubbles as a practical technology for manufacturing contrast agents for ultrasonic imaging. *Lab Chip* **7**, 463–468. (doi:10.1039/b701481n)

Jayasinghe, S. N. & Edirisinghe, M. J. 2002 Effect of viscosity on the size of relics produced by electrostatic atomization. *J. Aerosol Sci.* **33**, 1379–1388. (doi:10.1016/S0021-8502(02)00088-5)

Klibanov, A. L., Hughes, M. S., Wojdyla, J. K., Wible, J. H. & Brandenburger, G. H. 2002 Destruction of contrast agent microbubbles in the ultrasound field: the fate of the microbubble shell and the importance of the bubble gas content. *Acad. Radiol.* **9**, S41–S45. (doi:10.1016/S1076-6332(03)80393-8)

Krasovitski, B. & Kimmel, E. 2006 Stability of an encapsulated bubble shell. *Ultrasonics* **44**, 216–220. (doi:10.1016/j.ultras.2005.11.003)

Ku, B. K. & Kim, S. S. 2002 Electrospray characteristics of highly viscous liquids. *J. Aerosol Sci.* **33**, 1361–1378. (doi:10.1016/S0021-8502(02)00075-7)

Lopez-Herrera, J. M., Barrero, A., Lopez, A., Loscertales, I. G. & Marquez, M. 2003 Coaxial jets generated from electrified Taylor cones. Scaling laws. *J. Aerosol Sci.* **34**, 535–552. (doi:10.1016/S0021-8502(03)00021-1)

Loscertales, I. G., Barrero, A., Guerrero, I., Cortijo, R., Marquez, M. & Ganan-Calvo, A. M. 2002 Micro/nano encapsulation via electrified coaxial liquid jets. *Science* **295**, 1695–1698. (doi:10.1126/science.1067595)

Pancholi, K., Stride, E. & Edirisinghe, M. J. 2008 Dynamics of bubble formation in highly viscous liquids. *Langmuir* **24**, 4388–4393. (doi:10.1021/la703849x)

Raisinghani, A. & DeMaria, A. N. 2002 Physical principles of microbubble ultrasound contrast agents. *Am. J. Cardiol.* **90**, 3J–7J. (doi:10.1016/S0002-9149(02)02858-8)

Soetanto, K. & Chan, M. 2000 Study on the lifetime and attenuation properties of microbubbles coated with carboxylic acid salts. *Ultrasonics* **38**, 969–977. (doi:10.1016/S0041-624X(00)00027-5)

Stride, E. & Saffari, N. 2003 Microbubble ultrasound contrast agents: a review. *Proc. Inst. Mech. Eng. Part H: J. Eng. Med.* **217**, 429–447. (doi:10.1243/09544110360729072)

Stride, E. & Saffari, N. 2005 Investigating the significance of multiple scattering in ultrasound contrast agent particle populations. *IEEE Trans. Ultrason. Ferroelectr. Freq. Control* **52**, 2332–2345. (doi:10.1109/TUFFC.2005.1563278)

Stride, E., Pancholi, K., Edirisinghe, M. J. & Samarasinghe, S. 2008 Increasing the nonlinear character of microbubble oscillations at low acoustic pressures. *J. R. Soc. Interface* **5**, 807–811. (doi:10.1098/rsif.2008.0005)

Talu, E., Lozano, M. M., Powell, R. L., Dayton, P. A. & Longo, M. L. 2006 Long-term stability by lipid coating monodisperse microbubbles formed by a flow-focusing device. *Langmuir* **22**, 9487–9490. (doi:10.1021/la062095+)

Unger, E. C., Porter, T., Culp, W., Labell, R., Matsunaga, T. & Zutshi, R. 2004 Therapeutic applications of lipid-coated microbubbles. *Adv. Drug Deliv. Rev.* **56**, 1291–1314. (doi:10.1016/j.addr.2003.12.006)

Wang, W. H., Moser, C. C. & Weatley, M. A. 1996 Langmuir trough study of surfactant mixtures used in the production of a new ultrasound contrast agent consisting of stabilized microbubbles. *J. Phys. Chem.* **100**, 13 815–13 821. (doi:10.1021/jp9613549)